Scientia Iranica A (2015) 22(6), 2052–2060

Sharif University of Technology
Scientia Iranica
Transactions A: Civil Engineering
www.scientiairanica.com

Plunging breaker model of solitary wave with arbitrary Lagrangian Eulerian approach using mapping techniques

A. Lohrasbi* **and M.D. Pirooz**

Department of Civil Engineering, University of Tehran, Tehran, Iran.

Received 12 January 2015; received in revised form 15 February 2015; accepted 9 March 2015

KEYWORDS
Wave breaking;
Solitary waves;
Mapping;
Navier-stokes equations;
Plunging;
Arbitrary Lagrangian Eulerian.

Abstract. Better understanding and modeling of breaking waves are critical issues for coastal engineering. This article concerns the plunging wave break with free surface over a slope bottom considering unsteady, incompressible viscous flow. The method solves the two-dimensional Navier-Stokes equations for conservation of momentum, continuity equation, and full nonlinear kinematic free-surface equation for Newtonian fluids as the governing equations in a vertical plane. A new mapping was developed to trace the deformed free surface encountered during wave propagation by transferring the governing equations from the physical domain to a computational domain. Also, a numerical scheme is developed using finite element modeling technique to predict the plunging wave break. The Arbitrary Lagrangian Eulerian (ALE) algorithm is employed in modeling wave propagation over sloping beaches. In the conclusion, results are compared with the results of other researches.

1. Introduction

Breaking waves have strong effects on the hydrodynamic behavior of ship wakes as well as on the structural behavior of offshore structures. Depending on the way in which they break, breaking waves have been classified as spilling, plunging, surging, or collapsing. Plunging breakers are the major causes of overturning of ships in rough seas. Before Longuet and Cokelet [1], most of the numerical computations had succeeded only in integrating the equations of motion up to the instant when surface became vertical. Wellford and Ganaba [2], using finite element techniques, analyzed free surface problems involving extra-large free surface motions. They employed a spatially fixed Eulerian mesh in regard to the moving Lagrangian free surface line. Fenton and Rienecker [3] have developed the Fourier method to address the interaction of solitary waves with an impermeable wall, whereas Kim et al. [4] used the Boundary Integral Equation Method (BIEM) for the same problem. Zelt [5] parameterized wave breaking with an artificial viscosity term in the momentum equation to damp-out the oscillation of free surface right behind the bore. Furthermore, Zelt [6] investigated the run-ups of nonbreaking and breaking solitary waves on plane impermeable beaches by using his Boussinesq wave model and a Lagrangian finite element method. Solitary wave generation, propagation, and run-up are well described, and forces for a vertical wall case are also calculated in their method. Hayashi et al. [7] applied a finite element analysis on the Lagrangian description, combined with a fractional step method to solve unsteady incompressible viscous fluid flow governed by Navier-Stokes equations. Using the same model, they also simulated the solitary wave run-up on a circular island. Dolatshahi and Wellford [8] analyzed free surface profile with a two-dimensional Arbitrary Lagrangian-Eulerian finite element method

*. *Corresponding author. Tel.: +98 21 44258217*
E-mail addresses: ar_lohrasbi@ut.ac.ir (A. Lohrasbi); mdolat@ut.ac.ir (M.D. Pirooz)

to predict wave breaking. They computed the wave run-up over the vertical wall by employing Eulerian description in wave propagation direction and Lagrangian description in vertical direction. Oscillation of the free surface on the vertical wall due to mesh movement in the x direction was a deficiency in this method. Detailed characteristics of solitary waves shoaling over plane slopes and those of solitary wave breakers, like jet shape and wave height variation, were studied by Grilli et al. [9]. Titov and Synolakis [10] have extended viscid solution to two-dimensional topographies and solved several large-scale problems. Zhou and Stansby [11] extended an Arbitrary Lagrangian-Eulerian model in the σ coordinate system (ALE σ) for shallow water flows, based on the unsteady Reynolds-averaged Navier-Stokes equations. Gaston and Kamara [12] presented a two-dimensional Lagrangian-Eulerian finite element approach for the non-steady state turbulent fluid flows with free surfaces. Their model was based on a velocity-pressure finite element Navier-Stokes solver, including an augmented Lagrangian technique. Turbulent effects were taken with the $k-\varepsilon$ two-equation statistical model. Mesh was updated using an Arbitrary Lagrangian-Eulerian (ALE) method for a proper description of the free surface evolution. Dyachenko et al. [13] used conformal mapping method for free surface waves. They solved the potential flow of two-dimensional ideal incompressible fluid with a free surface using the theory of conformal mappings and Hamiltonian formalism and they reached the exact equations. Li et al. [14] studied the exact evolution equations for surface waves in water of finite depth using conformal mapping. Zakharov et al. [15] presented a new method for numerical simulation of a non-stationary potential flow of incompressible fluid with free surface of two-dimensional fluid, based on combination of the conformal mapping and Fourier Transform. The method is efficient for study of strongly nonlinear effects in gravity waves including wave breaking and formation of rogue waves. Klopman [16] proposed the variational Boussinesq model for solitary wave and represented free surface overturning using Fourier transformation. Ginnis et al. [17] matched the collocated Boundary Element Methods (BEM) with the unstructured analysis suitable for T-spline surfaces to solve free surface problems such as wave breaking.

For the present study, flow is assumed to be viscous and incompressible. No artificial viscosity is introduced in the kinematic free surface equations for out of the free surface oscillations in the region. The equations of conservation of momentum and mass for incompressible Newtonian fluids given by Navier-Stokes along with the fully nonlinear kinematic free surface equation are adopted as the governing equations. A particular mapping technique is used to transform the fluid region and its boundaries into a regular geometry for a convenient treatment of the moving free surface and irregular bottom topography. So it leads to transformation of the governing equations and the boundary conditions into more complicated equations. However, the transformed equations can be effectively handled by a proper analytical and numerical procedure. Validity of the proposed algorithms are examined by comparing the results with the available numerical approaches to experimental results.

2. Free surface flow

The high order theory is required to address the nonlinearity effects of extra-large free surface displacements. Navier-Stokes equations are suitable for a variety of problems in fluid mechanics, including extra-large free surface displacements, and have been used in different methods by researchers in this field.

2.1. Problem formulation

The physical domain $\bar{V}$ surrounded by a piecewise smooth boundary $\bar{S}$ is shown in Figure 1. This domain is occupied by a viscous incompressible fluid with the coefficients of constant kinematic viscosity (v) and specific mass (ρ). The problem under consideration is unsteady motion of a surface wave under gravity; also, two-dimensional unsteady incompressible viscous flow is considered. The governing equations are expressed by the unsteady Navier-Stokes equation and the equation of continuity. The rectangular coordinates are denoted by x, y, and the corresponding velocity components are denoted by $\bar{u}$ and $\bar{v}$. As a result, the equations of conservation of momentum and mass, for incompressible Newtonian fluids, in the arbitrary Lagrangian-Eulerian form are given as follows:

$$\frac{\partial \bar{u}}{\partial \bar{t}}|_{x,y} + (\bar{u} - \bar{w}_v)\frac{\partial \bar{u}}{\partial \bar{x}} + (\bar{v} - \bar{w}_v)\frac{\partial \bar{u}}{\partial \bar{y}} = -\frac{1}{\rho}\frac{\partial \bar{p}}{\partial \bar{x}} + \bar{v}\left(\frac{\partial^2 \bar{v}}{\partial \bar{x}^2} + \frac{\partial^2 \bar{u}}{\partial \bar{y}^2}\right),$$

$$\frac{\partial \bar{v}}{\partial \bar{t}}|_{x,y} + (\bar{u} - \bar{w}_v)\frac{\partial \bar{v}}{\partial \bar{x}} + (\bar{v} - \bar{w}_v)\frac{\partial \bar{v}}{\partial \bar{y}} = -\frac{1}{\rho}\frac{\partial \bar{p}}{\partial \bar{y}} + \bar{v}\left(\frac{\partial^2 \bar{v}}{\partial \bar{x}^2} + \frac{\partial^2 \bar{v}}{\partial \bar{y}^2}\right) - \bar{g},$$

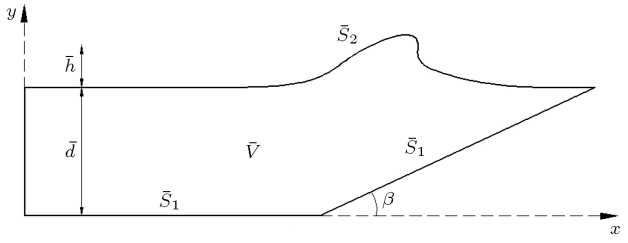

Figure 1. Mathematical models for non-linear analysis.

$$\frac{\partial \bar{u}}{\partial \bar{x}} + \frac{\partial \bar{v}}{\partial \bar{y}} = 0, \tag{1}$$

where $\bar{w}_u$ and $\bar{w}_v$ are the mesh velocities in x and y directions. The boundary $\bar{S}$ consists of two types of boundaries: One is the $\bar{S}_1$ on which velocity is given, the other is the free surface boundary $\bar{S}_2$ on which the surface force is specified. The boundary conditions can be expressed as the followings:

$$\bar{u} = \hat{\bar{u}} \quad \text{on} \quad \bar{S}_1$$

$$\left(-\frac{1}{\bar{\rho}}\bar{p} + 2\bar{v}\frac{\partial \bar{u}}{\partial \bar{x}}\right).n_{\bar{x}} + \bar{v}\left(-\frac{\partial \bar{u}}{\partial \bar{y}} + \frac{\partial \bar{v}}{\partial \bar{x}}\right).n_{\bar{y}} = \hat{\bar{c}}_x \quad \text{on} \quad \bar{S}_2$$

$$\bar{v} = \hat{\bar{v}} \quad \text{on} \quad \bar{S}_1$$

$$\bar{v}\left(\frac{\partial \bar{u}}{\partial \bar{y}} + \frac{\partial \bar{v}}{\partial \bar{x}}\right).n_{\bar{x}} + \left(-\frac{1}{\bar{\rho}}\bar{p} + 2\bar{v}\frac{\partial \bar{v}}{\partial \bar{y}}\right).n_{\bar{y}} = \hat{\bar{c}}_y \quad \text{on} \quad \bar{S}_2, \tag{2}$$

where the superscript caret denotes a function which is given on the boundary and $n_{\bar{x}}$ and $n_{\bar{y}}$ symbolize the direction cosines of outward normal to the boundary with respect to coordinates x and y. Also, $\hat{\bar{c}}_x$ and $\hat{\bar{c}}_y$ are the constants of integration. Top equations can be rendered dimensionless by introducing the following variables:

$$\bar{x} = x\bar{d}, \quad \bar{y} = y\bar{d}, \quad \bar{p} = p\bar{\rho}g\bar{d},$$

$$\bar{u} = u(\bar{g}\bar{d})^{1/2}, \quad \bar{v} = v(\bar{g}\bar{d})^{1/2}, \quad \bar{t} = t\left(\frac{\bar{d}}{\bar{g}}\right)^{1/2}. \tag{3}$$

Using these transformations, Eqs. (1) and (2) are modified as follows:

$$\frac{\partial u}{\partial t}|_{\xi,\eta} + (u - w_u)\frac{\partial u}{\partial x} + (v - w_v)\frac{\partial u}{\partial y} = -\frac{\partial p}{\partial x} + \frac{1}{\mathrm{Re}}\left(\frac{\partial^2 u}{\partial x^2} + \frac{\partial^2 u}{\partial y^2}\right),$$

$$\frac{\partial v}{\partial t}|_{\xi,\eta} + (u - w_u)\frac{\partial v}{\partial x} + (v - w_v)\frac{\partial v}{\partial y} = -\frac{\partial p}{\partial y} + \frac{1}{\mathrm{Re}}\left(\frac{\partial^2 v}{\partial x^2} + \frac{\partial^2 v}{\partial y^2}\right) - 1,$$

$$\frac{\partial u}{\partial x} + \frac{\partial v}{\partial y} = 0, \tag{4}$$

$$u = \hat{u} \quad \text{on} \quad \bar{S}_1$$

$$\left(-p + \frac{2}{\mathrm{Re}}\frac{\partial u}{\partial x}\right).n_x + \frac{1}{\mathrm{Re}}\left(\frac{\partial u}{\partial y} + \frac{\partial v}{\partial x}\right).n_y = \hat{c}_x \quad \text{on} \quad \bar{S}_2$$

$$v = \hat{v} \quad \text{on} \quad \bar{S}_1$$

$$\frac{1}{\mathrm{Re}}\left(\frac{\partial u}{\partial y} + \frac{\partial v}{\partial x}\right).n_x + \left(p + \frac{2}{\mathrm{Re}}\frac{\partial v}{\partial y}\right).n_y = \hat{c}_y \quad \text{on} \quad \bar{S}_2. \tag{5}$$

3. Solitary wave propagation

A solitary wave is essentially a wave that has infinite length lying entirely above the still-water level and propagates at a constant velocity without any change in form over a constant depth. Solitary waves are believed to represent a good model for both tsunamis and extreme design waves because of their large run-up, impulse, and impact force on structures. According to this characteristic that the wave keeps its initial form without deformation, the Eulerian Lagrangian description of fluid motion is employed here to solve the problem. In this description, the particles are followed in y direction in Lagrangian manner and the coordinate is fixed in the x direction. Although the solitary wave can be readily produced in laboratory, which appears to be the pure form, many numerical methods have failed to establish a wave of permanent shape. There are three theoretical solutions of the solitary wave equations. Boussinesq [18] obtained an analytical solution for the wave profile, wave propagation speed, and water particle velocities. The solution of Laitone [19] is similar to that of Boussinesq, but with higher order terms. He presented initial conditions and first approximations that are in the following dimensionless form:

$$h = H\mathrm{sech}\left[x\sqrt{.75h_0}\right],$$

$$v = yh\sqrt{3H}\tanh\left[x\sqrt{.75h_0}\right]$$

$$c = \sqrt{1+h} \qquad p = 1 + h - y \qquad u = h, \tag{6}$$

where c, u, v, p, y, and h denote normalized wave celerity, velocities in x and y directions, pressure, water depth, and wave height of the still-water surface, respectively. H stands for the maximum initial wave height of the incidental solitary wave.

4. Transformation of the basic equations into the mapped coordinate system

Computation of the propagation of free surface waves involves computational boundaries that do not coincide with coordinate lines in physical space. For the finite element method, such a problem requires a complicated interpolation function on the local grid lines which results in the local loss of accuracy in the computational solution. Such difficulties require a mapping or

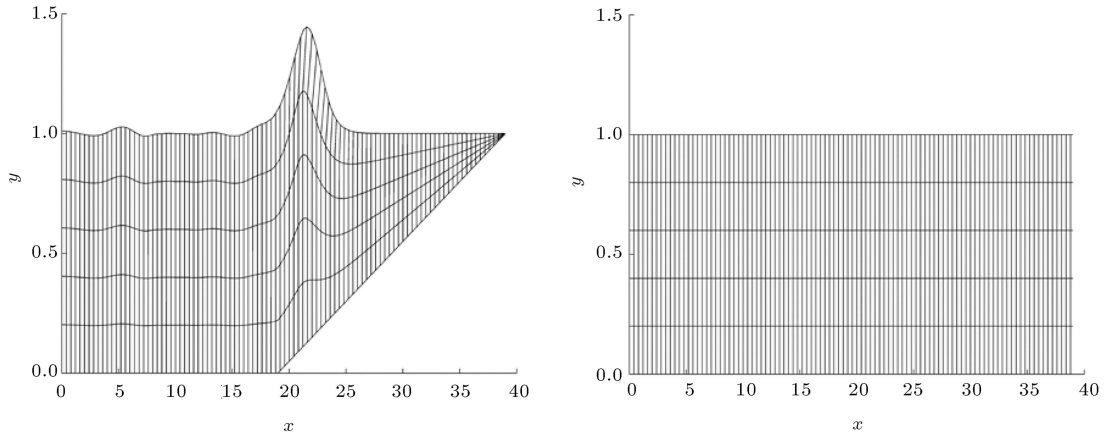

Figure 2. The computational grid is shown mapped back to the physical space.

transformation from physical space to a generalized space. This transformation simplifies the problem of highly deformed air-fluid interface that arises in the analysis of wave breaking. This mapping transforms the wave propagation model from the physical domain (x, y) to a computational domain (ξ, η). The use of generalized coordinates implies that a distorted region in physical space, such as breaking wave, is mapped into a rectangular region in the generalized coordinate space, where the unknown interface coincides with a coordinate line as in Figure 2.

Since the interior points in the computational domain form a regular grid and the boundaries coincide with coordinate lines, determination of $x(\xi, \eta)$ and $y(\xi, \eta)$ is easier than working in the irregular physical domain. The simple equation $x = \xi + h$ transforms physical to computational domain if free surface has no overturning (Figure 2). For mapping the overturned free surface and plunging wave breaker, the following mapping can be established:

$$x = \sum_{i=1}^{n} (\xi + h\alpha_i)\, F_i(\eta),$$

$$y = \eta(1 + h) + (1 - \eta)(\xi - \xi_s) \tan\beta, \tag{7}$$

where ξ_s is the starting point of slope; and $F_i(\eta)$ is the interpolation function employing n points in depth and it is the vital part of modelling. Accuracy of the model depends on the number of points in depth interpolation function.

$$F_i(\eta) = \sum_{j=1}^{n} b_{i,j}\eta^j, \tag{8}$$

where:

$$b_{i,j} = [c_{i,j}]^{-1} \times d_i, \tag{9}$$

and:

$$C = \lfloor c_{i,j} \rfloor_{n\times n}. \tag{10}$$

C has a matrix form such as:

$$C = \begin{bmatrix} 0 & 0 & \cdots \\ \left(\frac{1}{n-1}\right)^{n-1} & \left(\frac{1}{n-1}\right)^{n-2} & \cdots \\ \left(\frac{2}{n-1}\right)^{n-1} & \left(\frac{2}{n-1}\right)^{n-2} & \cdots \\ \cdots & \cdots & \cdots \\ \left(\frac{n-2}{n-1}\right)^{n-1} & \left(\frac{n-2}{n-1}\right)^{n-2} & \cdots \\ 1 & 1 & 1 \end{bmatrix}$$

$$\begin{bmatrix} 0 & 0 & 1 \\ \left(\frac{1}{n-1}\right)^{2} & \left(\frac{1}{n-1}\right) & 1 \\ \left(\frac{2}{n-1}\right)^{2} & \left(\frac{2}{n-1}\right) & 1 \\ \cdots & \cdots & 1 \\ \left(\frac{n-2}{n-1}\right)^{2} & \left(\frac{n-2}{n-1}\right)^{1} & 1 \\ 1 & 1 & 1 \end{bmatrix}_{n\times n}$$

$$= \left[\left(\frac{i-1}{n-1}\right)^{n-j}\right]_{n\times n} \tag{11}$$

that:

$$c_{i,j} = \left(\frac{i-1}{n-1}\right)^{n-j}, \tag{12}$$

and:

$$D = [d_{i,j}]_{n\times 1} = \lfloor 0^{j-i} \rfloor_{n\times 1}$$

$$= \lfloor 0^{1-i} \;\; 0^{2-i} \;\; \cdots 0^{n-1+i} \;\; 0^{n-i} \rfloor_{1\times n}. \tag{13}$$

Thus:

$$b_{i,j} = \left[\left(\frac{i-1}{n-1}\right)^{n-j}\right]^{-1}_{n\times n} \times \left[0^{i-j}\right]_{n\times 1}, \quad (14)$$

and finally:

$$F_i(\eta) = \left[\eta^{n-j}\right]_{1\times n} \times \left[\left(\frac{i-1}{n-1}\right)^{n-j}\right]^{-1}_{n\times n} \times \left[0^{i-j}\right]_{n\times 1}. \quad (15)$$

For example, interpolation functions employing three, four, and five points are presented in Eqs. (16) to (18):

$$\begin{aligned} F_1(\eta) &= 1 - 3\eta + 2\eta^2, \\ F_2(\eta) &= 4\eta - 4\eta^2, \\ F_3(\eta) &= -\eta + 2\eta^2, \end{aligned} \quad (16)$$

$$\begin{aligned} F_1(\eta) &= -4.5\eta^3 + 9\eta^2 - 5.5\eta^2 + 1, \\ F_2(\eta) &= 13.5\eta^3 - 22.5\eta^2 + 9\eta^2, \\ F_3(\eta) &= -13.5\eta^3 + 18\eta^2 - 4.5\eta^2, \\ F_4(\eta) &= 4.5\eta^3 - 4.5\eta^2 + \eta^2, \end{aligned} \quad (17)$$

$$\begin{aligned} F_1(\eta) &= 10.67\eta^4 - 26.67\eta^3 + 23.33\eta^2 - 8.33\eta + 1, \\ F_2(\eta) &= -42.67\eta^4 + 96\eta^3 - 69.33\eta^2 + 16\eta, \\ F_3(\eta) &= 64\eta^4 - 128\eta^3 + 76\eta^2 - 12\eta, \\ F_4(\eta) &= -42.67\eta^4 + 74.67\eta^3 - 37.33\eta^2 + 5.33\eta, \\ F_5(\eta) &= 10.67\eta^4 - 16\eta^3 + 7.33\eta^2 - \eta. \end{aligned} \quad (18)$$

For more accuracy, six point interpolation functions can be used as in Eq. (19) shown in Figure 3. It will be shown later that it is not necessary to use more points in interpolation functions.

$$\begin{aligned} F_1(\eta) &= -26.04\eta^5 + 78.13\eta^4 - 88.54\eta^3 + 46.88\eta^2 \\ &\quad -11.42\eta + 1, \\ F_2(\eta) &= 130.21\eta^5 - 364.58\eta^4 + 369.79\eta^3 - 160.42\eta^2 \\ &\quad +25.00\eta, \\ F_3(\eta) &= -260.42\eta^5 + 677.08\eta^4 - 614.58\eta^3 + 222.92\eta^2 \\ &\quad -25.00\eta, \\ F_4(\eta) &= 260.42\eta^5 - 625.00\eta^4 + 510.42\eta^3 - 162.50\eta^2 \\ &\quad +16.67\eta, \end{aligned}$$

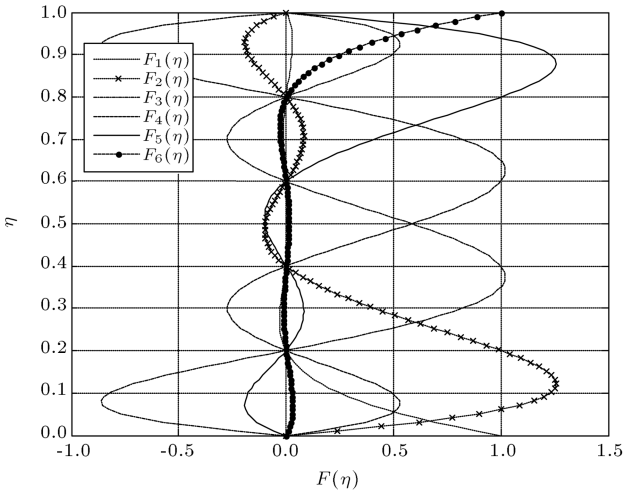

Figure 3. Six point interpolation function.

$$\begin{aligned} F_5(\eta) &= -130.21\eta^5 + 286.46\eta^4 - 213.54\eta^3 + 63.54\eta^2 \\ &\quad -6.25\eta, \\ F_6(\eta) &= 26.04\eta^5 - 52.08\eta^4 + 36.46\eta^3 - 10.42\eta^2 + \eta. \end{aligned} \quad (19)$$

The strategy to determine when the wave profile is not uniquely defined requires the calculation of Jacobin matrix of transportation. To have a single-value mapping and one-to-one mapping, the Jacobin matrix of transportation must be finite and non zero ($|J^{-1}| > 0$).

4.1. Eulerian description

To have an Eulerian description, where the physical coordinate system coincides with the generalized coordinate system, it is necessary to set $\alpha_i = \beta = h = 0$.

4.2. Eulerian description in x direction and Lagrangian description in y direction

Eulerian description in x direction and Lagrangian description in y direction can be applied for nonbreaking waves. In these cases, it is necessary to set $\alpha_i = 0$. The transformation is Lagrangian in y direction and Eulerian in x direction and the problems associated with this transformation should have a single value profile.

4.3. Arbitrary Lagrangian-Eulerian description

The arbitrary Lagrangian-Eulerian algorithm is employed in modelling wave propagation both over sloping beaches, where the evolution occurs over bathymetry topography, and over constant depth regions. Although this transformation is convenient for breaking waves, nonbreaking waves can also be treated using the same mapping. Various types of α_i depend on the nature of the problem. To coincide physical boundary with computational boundary, the α_i values are considered

to be a fifth order polynomial function of ξ as follows:

$$\alpha_i = f(\xi) = m_1\xi^5 + m_2\xi^4 + m_3\xi^3 + m_4\xi^2 + m_5\xi + m_6. \quad (20)$$

The coefficient m_i is calculated from these free surface conditions:

$$\begin{aligned}
&\xi = 0 \quad \Rightarrow \quad \alpha_i = 0,\\
&\xi = 0 \quad \Rightarrow \quad \frac{\partial \alpha_i}{\partial \xi} = 0,\\
&\xi = l \quad \Rightarrow \quad \alpha_i = 0,\\
&\xi = l \quad \Rightarrow \quad \frac{\partial \alpha_i}{\partial \xi} = 0,\\
&\xi = \varepsilon l \quad \Rightarrow \quad \alpha_i = b,\\
&\xi = \varepsilon l \quad \Rightarrow \quad \frac{\partial \alpha_i}{\partial \xi} = 0.
\end{aligned} \quad (21)$$

And finally fifth order polynomial function is:

$$\alpha_i = \frac{b}{\varepsilon^3 l^5 (1-\varepsilon)^3}\Big[2(\xi-\xi_0)^5(2\varepsilon-1) + l(\xi-\xi_0)^4 (4-5\varepsilon-5\varepsilon^2) + 2l^2(\xi-\xi_0)^3(-1-\varepsilon+5\varepsilon^2) + l^3\varepsilon(\xi-\xi_0)^2(3-5\varepsilon)\Big], \quad (22)$$

$$\alpha_i = C\alpha_{i-1} \qquad 0 < C < 0.5. \quad (23)$$

Definitions of b, ε, l, and ξ_0 are illustrated in Figure 4. Parameter C is a constant coefficient and its value is obtained by trial and error to stabilize the problem.

4.4. Variation equations in the transformed domain

Spatial discretization of partial differential equations in the numerical model is based on a Galerkin finite element method. This method is implemented using the weighted residual variation method for the solution within each element. Using standard linear shape-functions for a rectangular element in the natural coordinate system, the velocity, pressure, and correction potential fields within the element are interpolated in terms of their nodal values as follows:

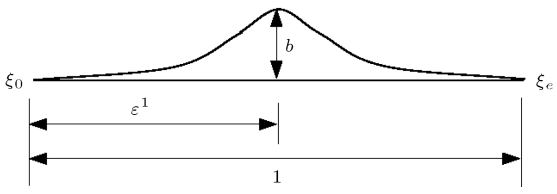

Figure 4. Parameters in α_i function.

$$u = \psi_\alpha u_\alpha, \qquad v = \psi_\alpha v_\alpha,$$
$$p = \psi_\alpha p_\alpha, \qquad \phi = \psi_\alpha \phi_\alpha, \qquad h = \psi_{\alpha s} h_\alpha, \quad (24)$$

where ψ_α is the interpolation function and u, v, ϕ, and h represent the nodal values at the node of the jth element. ϕ is the correction potential based on the Fractional step method presented by Hayashi and Hatanaka [20]. By dividing the total time of t into a number of short time increments of Δt, the equations of motion, continuity, and kinematic boundary condition can be discretized into:

$$\begin{aligned}
M_{\alpha\beta}\left|J^{-1}\right|^{n+1}\tilde{u}_\beta^{n+1} &= M_{\alpha\beta}\left|J^{-1}\right|^n u_\beta^n \\
&- \frac{\Delta t}{\mathrm{Re}}\left[\left[\left(\frac{\partial \xi^n}{\partial x}\right)^2 + \left(\frac{\partial \xi^n}{\partial y}\right)^2\right] M_{\alpha 1\beta 1}\right. \\
&+ \left[2\left(\frac{\partial \eta^n}{\partial x}\right)^2 + \left(\frac{\partial \eta^n}{\partial y}\right)^2\right] M_{\alpha 2\beta 2} \\
&\left. + \left(2\frac{\partial \xi^n}{\partial x}\frac{\partial \eta^n}{\partial x} + \frac{\partial \xi^n}{\partial y}\frac{\partial \eta^n}{\partial y}\right)\left(M_{\alpha 1\beta 2} + M_{\alpha 2\beta 1}\right)\right] \\
&\left|J^{-1}\right|^n u_\beta^n - \frac{\Delta t}{\mathrm{Re}}\left(\frac{\partial \xi^n}{\partial x}\frac{\partial \xi^n}{\partial y} M_{\alpha 1\beta 1}\right. \\
&+ \frac{\partial \xi^n}{\partial y}\frac{\partial \eta^n}{\partial x} M_{\alpha 1\beta 2} + \frac{\partial \eta^n}{\partial y}\frac{\partial \xi^n}{\partial x} M_{\alpha 2\beta 1} \\
&\left. + \frac{\partial \eta^n}{\partial x}\frac{\partial \eta^n}{\partial y} M_{\alpha 2\beta 2}\right)\left|J^{-1}\right|^n v_\beta^n \\
&- \Delta t\left[\left(\frac{\partial \xi^n}{\partial x} M_{\alpha 1\beta\beta 1} + \frac{\partial \eta^n}{\partial x} M_{\alpha\beta\beta 2}\right)\left({u_\beta}^n - {w_u}_\beta^n\right)\right. \\
&\left. + \left(\frac{\partial \xi^n}{\partial y} M_{\alpha\beta\beta 1} + \frac{\partial \eta^n}{\partial y} M_{\alpha\beta\beta 2}\right)\left({v_\beta}^n - {w_v}_\beta^n\right)\right] \\
&\left|J^{-1}\right|^n {u_\beta}^n + \Delta t\left(\frac{\partial \xi^n}{\partial x} M_{\alpha 1\beta} + \frac{\partial \eta^n}{\partial x} M_{\alpha 2\beta}\right)\left|J^{-1}\right|^n p_\beta^n,
\end{aligned} \quad (25)$$

$$M_{\alpha\beta}\left|J^{-1}\right|^{n+1} u_\beta^{n+1} = M_{\alpha\beta}\left|J^{-1}\right|^{n+1}\tilde{u}_\beta^{n+1} + \left(\frac{\partial \xi^{n+1}}{\partial x} M_{\alpha\beta 1} + \frac{\partial \eta^{n+1}}{\partial x} M_{\alpha\beta 2}\right)\left|J^{-1}\right|^{n+1}\phi_\beta, \quad (26)$$

$$M_{\alpha\beta}\left|J^{-1}\right|^{n+1} v_\beta^{n+1} = M_{\alpha\beta}\left|J^{-1}\right|^{n+1}\tilde{v}_\beta^{n+1} + \left(\frac{\partial \xi^{n+1}}{\partial y} M_{\alpha\beta 1} + \frac{\partial \eta^{n+1}}{\partial y} M_{\alpha\beta 2}\right)\left|J^{-1}\right|^{n+1}\phi_\beta, \quad (27)$$

$$M_{\alpha\beta}\left|J^{-1}\right|^{n+1}p_\beta^{n+1}=M_{\alpha\beta}\left|J^{-1}\right|^{n}p_\beta^{n}-\frac{1}{\Delta t}M_{\alpha\beta}\left|J^{-1}\right|^{n+1}\phi_\beta, \quad (28)$$

$$H_{\alpha\beta}\left|J_s^{-1}\right|^{n+1}h_\beta^{n+1}=H_{\alpha\beta}\left|J_s^{-1}\right|^{n}h_\beta^{n}+\Delta t\Big[H_{\alpha\beta}\left|J_s^{-1}\right|^{n+1}v_\beta{}^{n+1}-\left(\frac{\partial\xi^n}{\partial x}H_{\alpha\beta\beta1}+\frac{\partial\eta^n}{\partial x}H_{\alpha\beta\beta2}\right)\left(u_\beta^{n+1}-w_{u\beta}^{n+1}\right)\left|J_s^{-1}\right|^{n+1}h_\beta^{n}\Big]. \quad (29)$$

Note that due to the complexity, the equations are written in the mapped domain using indicial notation. $\left|J^{-1}\right|$ is the Jacobin inverse of transformation matrix and the following definitions are for the consistent mass matrix obtained from analytical integration used to write the above equations.

$$M_\alpha=\int_V\psi_\alpha dV,\quad M_{\alpha\beta\beta1}=\int_V\psi_\alpha\psi_\beta\frac{\partial\psi_\beta}{\partial\xi}dV,$$

$$M_{\alpha\beta}=\int_V\psi_\alpha\psi_\beta dV,\quad M_{\alpha\beta\beta2}=\int_V\psi_\alpha\psi_\beta\frac{\partial\psi_\beta}{\partial\eta}dV,$$

$$M_{\alpha1\beta1}=\int_V\frac{\partial\psi_\alpha}{\partial\xi}\frac{\partial\psi_\beta}{\partial\xi}dV,\quad H_{\alpha\beta}=\int_S\psi_\alpha\psi_\beta dS,$$

$$M_{\alpha1\beta2}=\int_V\frac{\partial\psi_\alpha}{\partial\xi}\frac{\partial\psi_\beta}{\partial\eta}dV,\quad H_{\alpha\beta1}=\int_S\psi_\alpha\frac{\partial\psi_\beta}{\partial\xi}dS,$$

$$M_{\alpha2\beta1}=\int_V\frac{\partial\psi_\alpha}{\partial\eta}\frac{\partial\psi_\beta}{\partial\xi}dV,\quad H_{\alpha\beta2}=\int_S\psi_\alpha\frac{\partial\psi_\beta}{\partial\eta}dS,$$

$$M_{\alpha\beta1}=\int_V\frac{\partial\psi_\alpha}{\partial\xi}\psi_\beta dV,\quad H_{\alpha\beta\beta1}=\int_S\psi_\alpha\psi_\beta\frac{\partial\psi_\beta}{\partial\xi}dS$$

$$M_{\alpha\beta2}=\int_V\psi_\alpha\frac{\partial\psi_\beta}{\partial\eta}dV,$$

$$H_{\alpha\beta\beta2}=\int_S\psi_\alpha\psi_\beta\frac{\partial\psi_\beta}{\partial\eta}dS. \quad (30)$$

It should be noted that all of the derivations are with respect to ξ_i.

5. Results

For showing the propagation and deformation of a solitary wave with Navier-Stokes equations, the physical domain with 1 m in depth and 40 m in length is discrete to $\Delta x=\Delta y=0.2$ m with 5×200 elements in space with $\Delta t=0.01$ Sec in time and the results have been shown in Figure 5. Figures 6 to 8 show the results of wave breaking with $H/ho=0.20$ on various slopes.

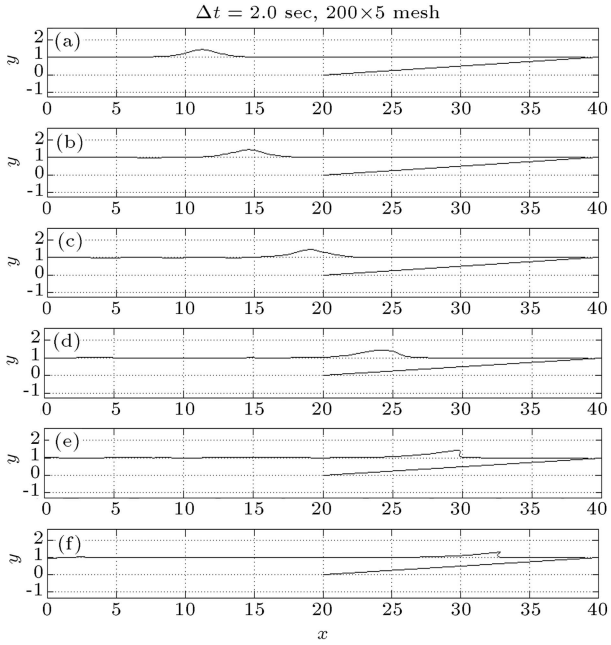

Figure 5. Solitary wave propagation with $H/ho=0.40$ on a bed with slope=0.05.

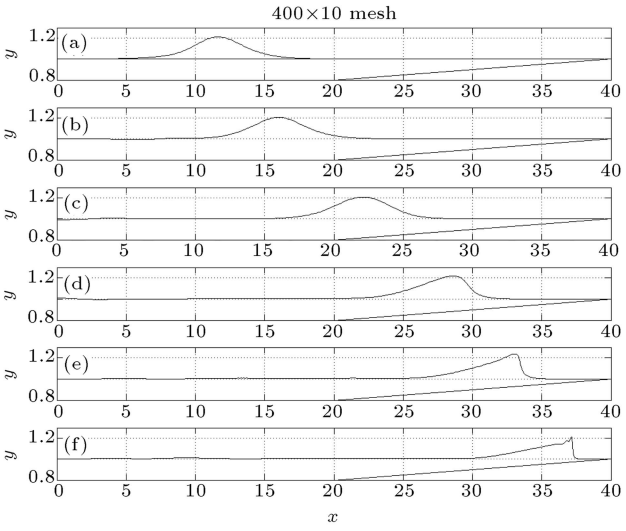

Figure 6. Solitary wave propagation with $H/ho=0.20$ on a bed with slope=0.05.

For better judgment about the efficiency and effectiveness of Arbitrary Lagrangian-Eulerian algorithm, the results of this numerical model have been compared with the shape obtained from the numerical results of Grilli et al. [9] and experimental results of Li [21] with $H/ho=0.30$ and $H/ho=0.45$ in Figures 9 and 10. In this method, nodal points can move in both coordinate directions by introducing appropriate mapping functions as defined in Eq. (7). The model is validated by comparing numerical results with other results.

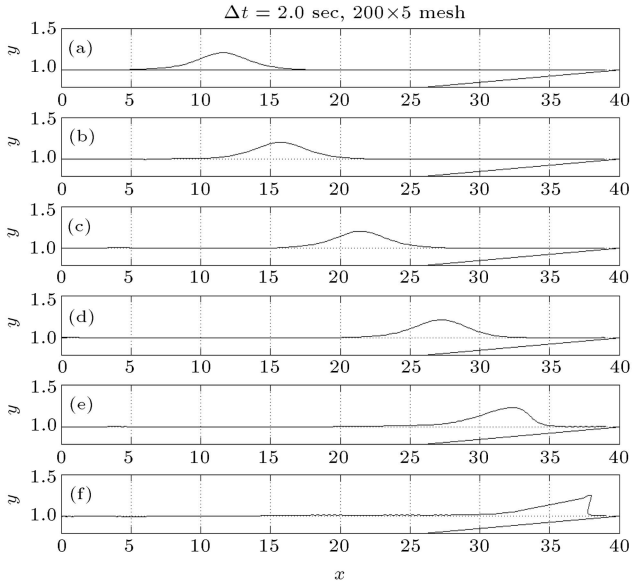

Figure 7. Solitary wave propagation with $H/ho = 0.20$ on a bed with slope=0.075.

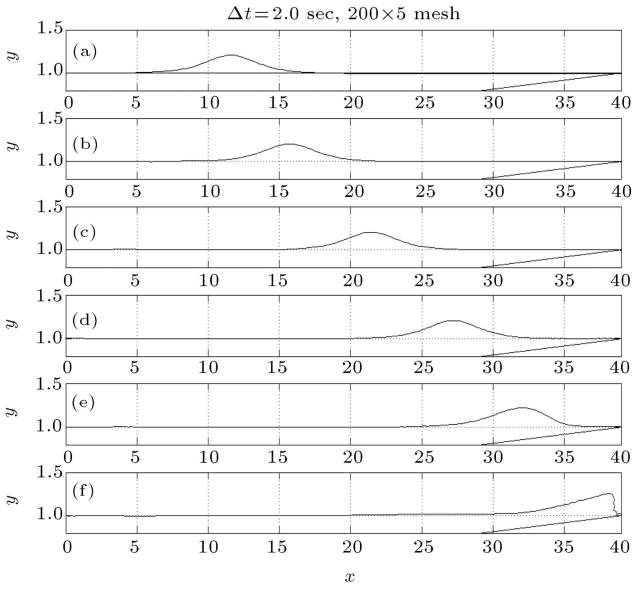

Figure 8. Solitary wave propagation with $H/ho = 0.20$ on a bed with slope=0.09.

6. Conclusion

The method involves a two-dimensional finite element to solve the Navier-Stokes equations. The free surfaces in previous research only reach vertical wall and they cannot show any overturning. So the mapping was developed to solve highly deformed free surface problems such as plunging breaker. The model was able to demonstrate the multi-valued surface when steepening of the forward face of wave passes the vertical position. Also this mapping can transform any bathymetry from the physical domain to the computational domain. This mapping models the overturning wave, but cannot touch the frontier surface.

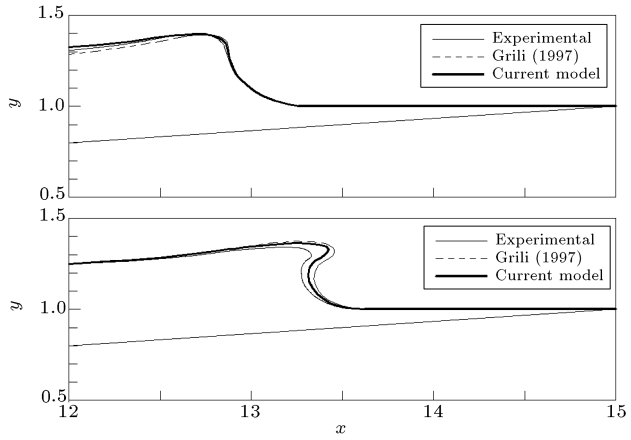

Figure 9. Comparison of the breaking wave shape obtained from numerical results of Grilli et al. [9] with experimental results of Li [21] and the current model ($H/ho = 0.30$ and slope=0.067).

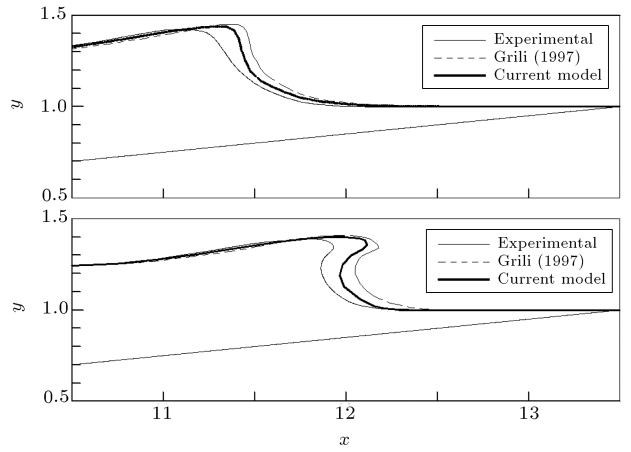

Figure 10. Comparison of the breaking wave shape obtained from numerical results of Grilli et al. [9] with experimental results of Li [21] and the current model ($H/ho = 0.45$ and slope=0.1).

It is almost a general method to handle different aspects of fluid mechanics problems. Another advantage of the present study is that no smoothing or artificial viscosity is applied. The model's convergence is satisfactory and contrasts to most of the other methods. The developed techniques could easily be extended to analyze other free surface problems such as dam break and hydraulic jump.

References

1. Longuet-Higgins, M.S. and Cokelet, E.D. "The deformation of steep surface waves on water. I. A numerical method of computation", *Proc. Royal Soc.*, **350**, pp. 1-26 (1976).
2. Wellford, C.L. and Ganaba, T.H. "A finite element

method with a hybrid Lagrangian line for fluid mechanics problems involving large free surface motion", *Int. Journal for Numerical Methods in Engineering.*, **17**, pp. 1201-1231 (1981).

3. Fenton, J.D. and Rienecker, M.M. "A Fourier method for solving nonlinear water-wave problems, application to solitary-wave interactions", *Journal of Fluid Mechanics*, **118**, pp. 411-443 (1982).
4. Kim, P.L., Liu, J.A. and Liggett, S.K. "Boundary integral equation solutions for solitary wave generation, propagation and run-up", *Coastal Engineering*, **7**, pp. 299-317 (1983).
5. Zelt, J.A., *The Response of Harbors with Sloping Boundaries to Long Wave Excitation*, California Institute of Technology, Pasadena., M. Keck Laboratory of Hydraulics and Water Resources (1986).
6. Zelt, J.A. "The run-up of non-breaking and breaking solitary waves", *Coastal Engineering*, **15**, pp. 205-246 (1991).
7. Hayashi, M., Hatanaka, K. and Kawahara, M. "Lagrangian finite element method for free surface Navier-Stokes flow using fractional step methods", *Int. Journal for Numerical Methods in Fluids*, **13**, pp. 805-840 (1991).
8. Dolatshahi P.M. and Wellford, C.L., *Finite Element Methods for Viscous Free Surface Fluids Including Breaking and Non-Breaking Waves*, University of Southern California California (1995).
9. Grilli, S.T., Svendsen, I.A. and Subramanya, R. "Breaking criterion and characteristics for solitary waves on slopes", *Journal of Waterway Port Coastal and Ocean*, **123**, pp. 102-112 (1997).
10. Titov, V. and Synolakis, C. "Numerical modeling of tidal wave runup", *Journal of Waterways, Port, Coastal and Ocean Engineering, ASCE*, **124**, pp. 157-171 (1998).
11. Zhou, J.G. and Stansby, P.K. "An arbitrary Lagrangian-Eulerian (ALE) model with non-hydrostatic pressure for shallow water flows", *Computer Methods in Applied Mechanics and Engineering*, **178**, pp. 199-214 (1998).
12. Gaston, L. and Kamara, A. "Arbitrary Lagrangian-Eulerian finite element approach to non-steady state turbulent fluid flow with application to mould filling in casting", *International Journal for Numerical Methods in Fluids*, **34**, pp. 341-369 (2000).
13. Dyachenko, A.I., Kuznetsov, E.A., Spector, M.D. and Zakharov, V.E. "Analytical description of the free surface dynamics of an ideal fluid (canonical formalism and conformal mapping)", *Phys. Lett. A*, **221**, pp. 73-79 (1996).
14. Li, Y.A., Hyman, J.M. and Choi, W.Y. "A numerical study of the exact evolution equations for surface waves in water of finite depth", *Studies in Applied Mathematics*, **113**, pp. 303-324 (2004).
15. Zakharov, V.E., Dyachenko, A.I. and Vasilyev, O.A. "New method for numerical simulation of a nonstationary potential flow of incompressible fluid with a free surface", *European Journal of Mechanics B/Fluids*, **21**, pp. 283-291 (2009).
16. Klopman, G. "Variational Boussinesq modelling of surface gravity waves over bathymetry", PhD Thesis, University of Twente, Twente (2010).
17. Ginnis, A.I. et al. "Isogeometric boundary-element analysis for the wave-resistance problem using T-splines", The Institute for Computational Engineering and Sciences, The University of Texas at Austin, ICES REPORT 14-03 (2014).
18. Boussinesq, J. "Theorical recherch on the flow rate of groundwater percolating in the soil and on the yield of springs in French" [Recherches théoriques sur l'écoulement des nappes d'eau infiltrées dans le sol et sur le débit des sources], *J. Math. Pure Appl.*, **10**, pp. 5-78 (1904).
19. Laiton, E.V. "The second approximation to cnoidal and solitary waves", *Journal of Fluid Mechanics*, **9**, pp. 430-444 (1960).
20. Hayashi, M., Hatanaka, K. and M.K. "Lagrangian element method for free surface Navier-Stokes flow using fractional step methods", *International Journal for Numerical Methods in Fluids*, **13**, pp. 805-840 (1991).
21. Li, Y. "Tsunamis: non-breaking and breaking solitary wave run-up", Technical Report, California Institute of Technology, Pasadena, CA. (2000).

Biographies

Alireza Lohrasbi received his PhD degree from the Department of Civil Engineering, University of Tehran, Iran. His interest is in tsunami research and numerical and analytical modeling of breaking waves. He has published several technical lectures in hydrodynamic and hydraulic modeling using Navier-Stokes equation.

Moharram D. Pirooz is an Associate Professor at the Department of Civil Engineering, University of Tehran, Iran. He is a very active engineer in the field of marine structures. He has published several technical lectures and worked with many consultants in hydrodynamic and hydraulic modeling. He has recently published two papers in the field of wave height prediction.